Spin Equilibrium in Five-co-ordinate Lewis-base Adducts of Cobalt(II) Schiff-base Complexes with a S_2N_3 Ligand Environment. Molecular and Crystal Structure of $[CoL^4(mim)]$ at 293 and 103 K [H_2L^4 = *N,N'*-bis(5-mercapto-3-methyl-1-phenylpyrazol-4-ylmethylene)-*o*-phenylenediamine, mim = *N*-methylimidazole] *

Alexander L. Nivorozhkin, Hans Toftlund and Max Nielsen
Department of Chemistry, Odense University, 5230 Odense M, Denmark

Four novel five-co-ordinate Lewis-base adducts of cobalt(II) Schiff-base complexes with a S_2N_3 ligand environment have been prepared and their variable-temperature magnetic susceptibilities determined (T = 77–300 K). The χ_{Co}^{-1} *vs.* T plots revealed a minimax behaviour characteristic of an $S = \frac{1}{2} \rightleftharpoons \frac{3}{2}$ spin equilibrium. The corresponding magnetic moments decrease in a gradual manner on lowering the temperature. The thermodynamic parameters for the equilibrium were estimated from the magnetic moment data and $\Delta H°$ values were found to lie in the range of 273–757 cm^{-1}. Decrease of the in-plane ligand field causes a decrease of the transition temperature and stabilization of the high-spin relative to the low-spin ground state. The X-ray single-crystal structural determinations for $[CoL^4(mim)]$ [H_2L^4 = *N,N'*-bis(5-mercapto-3-methyl-1-phenylpyrazol-4-ylmethylene)-*o*-phenylenediamine, mim = *N*-methylimidazole] were carried out at 293 (μ_{eff} = 3.6 μ_B) and 103 K (μ_{eff} = 2.3 μ_B). The co-ordination geometry around the cobalt centre revealed a distorted trigonal bipyramid with one N and one S atom of the metallocycle as axial ligands, and the other N,S atoms and the *N*-imidazole nitrogen situated in an equatorial plane. Comparison of the molecular structures at different temperatures indicates an occurrence of some configurational and conformational changes along with variations in metal–ligand bond lengths associated with a spin transition. Lowering the temperature results in increase of one of the N–Co–S valence angles by 7.2°, an increase in the Co–N(imidazole) bond length by 0.023 Å but decreases in the other metal–ligand bonds by 0.02–0.05 Å.

The electronic spin-crossover behaviour of transition-metal complexes has been of interest for the past decade in relation to the theoretical aspects of the problem, magnetic properties of metalloproteins and in the design of magnetic molecular materials.[1–6] In contrast to the extensively investigated iron-(II) and -(III) systems,[1–5] cobalt(II) complexes[2,6] are relatively unexplored. One of the few well documented examples concerning spin-crossover cobalt(II) complexes includes thermal-induced spin transition and spin equilibrium in five- and six-co-ordinated Lewis-base adducts of cobalt(II) chelates derived from the deprotonated form of the *N,N'*-bridged tetradentate Schiff base of salicylaldehyde.[6,7] An appropriate energy separation between doublet and quartet cobalt(II) (d^7) spin states of *ca.* 500 cm^{-1} required in fine-tuning spin interconversions was reported to be determined by a delicate balance of the nature of the in-plane ligand and the basicity and steric properties of the axially co-ordinated Lewis base, in this case nitrogen-containing heterocycles such as substituted pyridines and imidazoles.[7] Stabilization of the high-spin state relative to the low-spin ground state was found to be favoured when the corresponding pK_a values of the Lewis base increase. The *N,N'*-bridging group of the in-plane ligand was chosen as $-(CH_2)_2-$ or *o*-phenylene in order to avoid too strong stabilisation of the high-spin ground state.

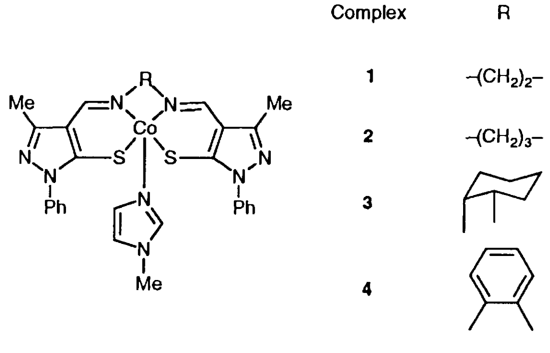

In this paper we report the syntheses and variable-temperature magnetic moment studies of novel Lewis-base adducts of cobalt(II) Schiff base complexes **1**–**4** with a CoS_2N_3 chromophore displaying spin equilibrium behaviour in the solid state. As a suitable Lewis base *N*-methylimidazole was selected. The in-plane ligand field was varied by changes in the *N,N'*-bridging fragment. Thus the purposes of the present study were: (*i*) to reveal any changes in the magnetic properties of complexes with a CoS_2N_3 chromophore compared to those of CoO_2N_3 type; (*ii*) to provide a more detailed insight into the influence of the in-plane ligand on the spin crossover behaviour and (*iii*) to ascertain structural changes associated with a low- to high-spin interconversion by single-crystal X-ray diffraction of one of the complexes in low- (103 K) and high-spin states (293 K).

Only two examples of variable-temperature molecular structures of spin-crossover cobalt(II) complexes have so far

---

* *Supplementary data available:* see Instructions for Authors, *J. Chem. Soc., Dalton Trans.*, 1994, Issue 1, pp. xxiii–xxviii.

Non-SI units employed: $cm^{-1} \approx 11.97\ J\ mol^{-1}$, $\mu_B \approx 9.274 \times 10^{-24}\ J\ T^{-1}$.

been reported, *viz.* [Co(nnp)(NCS)$_2$] [nnp = *N*-(diphenylphosphino)ethyl-*N*′,*N*′-diethylethylenediamine)[8,9] and [Co(terpy)$_2$]I$_2$·H$_2$O (terpy = 2,2′:6′,2″-terpyridine).[10]

Experimental

Physical Measurements.—Elemental analyses were carried out by the microanalytical laboratory at the H. C. Ørsted Institute, Copenhagen. Thermogravimetric curves were obtained using a SETARAM TG 92-12 thermobalance at a heating rate of 5 °C min^{-1} in a nitrogen atmosphere. Electronic impact mass spectra (70 eV, *ca.* 1.12 × 10^{-17} J) were recorded on a Varian Mat 311 A spectrometer and ^{1}H NMR spectra on a 250 MHz Bruker AC FT instrument, chemical shifts are reported relative to tetramethylsilane as internal standard. The EPR spectra were recorded at 77 K on a Varian E-LINE Century Series spectrometer operating at X-band frequency. Magnetic susceptibilities were measured by the Faraday method as previously described.[11] The molar susceptibilities were corrected for ligand diamagnetism using Pascal's constants.[12]

Synthesis of the Ligands H$_2$L^1–H$_2$L^4.—To a cooled slurry of Na$_2$S·*n*H$_2$O (*n* = 6–9) (20.0 g) in dimethyl sulfoxide (dmso) (40 cm^3) was added 5-chloro-4-formyl-3-methyl-1-phenylpyrazole (8.0 g, 36 mmol) with stirring. The reaction mixture was warmed at 60–70 °C for 3.5 h, then cooled and poured into ice-cold water (100 cm^3). After extraction with diethyl ether (75 cm^3) the water–dmso phase was placed in a separation funnel along with ether (100 cm^3) and 10% hydrochloric acid was added dropwise with shaking until no more precipitate appeared (pH 5–6). The ether layer was separated, washed with water (100 cm^3), dried over sodium sulfate and evaporated to dryness *in vacuo*. The resulting reddish oil was dissolved in absolute ethanol (130 cm^3) and the appropriate diamine (15 mmol) in ethanol (15 cm^3) was added dropwise under heating and the reaction mixture was refluxed until the condensation was completed (TLC control) for 1–2 h (H$_2$L^1–H$_2$L^3) or 18 h (H$_2$L^4) under nitrogen. After cooling the precipitated yellow solid was filtered off, washed with ethanol and dried *in vacuo*, yield 60–70%.

N,N′-*Bis*(5-*mercapto*-3-*methyl*-1-*phenylpyrazol*-4-*yl-methylene*)*ethylenediamine* H$_2$L^1. M.p. 279–280 °C (Found: C, 62.4; H, 5.4; N, 18.35; S, 13.9%; M^+, 460. C$_{24}$H$_{24}$N$_6$S$_2$ requires C, 62.6; H, 5.2; N, 18.3; S, 13.9%; *M*, 460); δ_H(CDCl$_3$) 2.15 (6 H, s, Me), 3.91 (4 H, m, CH$_2$), 7.28–7.78 (10 H, m, aryl H), 7.89 [2 H, d, ^3J(CH–NH) 8, NCH] and 13.1 [2 H, br d, ^3J(NH–CH) 8, NH].

N,N′-*Bis*(5-*mercapto*-3-*methyl*-1-*phenylpyrazol*-4-*yl-methylene*)*trimethylenediamine* H$_2$L^2. M.p. 196 °C [from toluene–acetonitrile (2:1)] (Found: C, 63.4; H, 5.6; N, 17.7%; M^+, 474. C$_{25}$H$_{26}$N$_6$S$_2$ requires C, 63.3; H, 5.5; N, 17.7%; *M*, 474); δ_H(CDCl$_3$) 2.29 (6 H, s, Me), 3.72 (4 H, m, CH$_2$), 7.2–7.8 (12 H, m, aryl H and NCH) and 13.15 (2 H, br, NH).

N,N′-*Bis*(5-*mercapto*-3-*methyl*-1-*phenylpyrazol*-4-*yl-methylene*)-cis-*cyclohexane*-1,2-*diamine* H$_2$L^3. M.p. 238–239 °C (Found: C, 63.9; H, 5.8; N, 16.95%; M^+, 514. C$_{28}$H$_{30}$N$_6$S$_2$·0.5H$_2$O requires C, 64.2; H, 5.9; N, 16.1%; *M*, 514); δ_H(CDCl$_3$) 1.60–1.80 (8 H, m, cyclohexyl), 2.06 (6 H, s, Me), 3.89 (2 H, m, cyclohexyl NCH), 7.20–7.90 (12 H, m, aryl H and NCH) and 13.38 (2 H, br s, NH).

N,N′-*Bis*(5-*mercapto*-3-*methyl*-1-*phenylpyrazol*-4-*yl-methylene*)-o-*phenylenediamine* H$_2$L^4. M.p. 167–169 °C (Found: C, 65.9; H, 4.8; N, 16.6%; M^+, 508. C$_{28}$H$_{24}$N$_6$S$_2$ requires C, 66.1; H, 4.8; N, 16.5%; *M*, 508); δ_H(CDCl$_3$) 2.35 (6 H, s, Me), 7.26–7.95 (14 H, m, aryl H), 8.15 [2 H, d, ^3J(CH–NH) 12, NCH] and 15.03 (2 H, br d, ^3J 12, CNH).

Synthesis of Cobalt Complexes.—All the complexes were synthesised according to the following general scheme using standard Schlenk glassware under a nitrogen atmosphere. The corresponding ligand (1 mmol) and *N*-methylimidazole (0.9 cm^3, 10 mmol) were dissolved in anhydrous dimethylformamide (3 cm^3) and cobalt(II) acetate tetrahydrate (250 mg, 1 mmol) was quickly added. The reaction mixture was refluxed for 15 min, and after cooling, methanol (5 cm^3) was added. A precipitate was filtered off and dried under a stream of nitrogen and then *in vacuo* at 45 °C overnight. The analytical data for complexes **1**–**4** are given in Table 1.

Crystal Structure Determination and Refinement.—Deep brown crystals of compound **4** suitable for single-crystal X-ray diffraction were deposited from the reaction mixture after 24 h at 25 °C. Diffraction data for **4** were collected with an Enraf-Nonius CAD4 diffractometer using graphite-monochromated Mo-Kα radiation. Crystal data and details of the data collection are given in Table 2. The intensity data were corrected for Lorentz and polarization effects and for absorption (ψ-scan). The structure was solved by direct methods using the program SHELXS 86[13a] and refined by full-matrix least-squares methods using the program SHELX 76.[13b] The carbon atoms were refined isotropically and other non-hydrogen atoms were assigned anisotropic thermal parameters. The positions of the hydrogen atoms were generated geometrically [*d*(C–H) 0.96 Å]. Atomic coordinates are given in Table 3 and bond lengths and angles in Table 4. The angles between selected planes are given in Table 5. The view of the molecule at 293 K is shown in Fig. 1.

Additional material available from the Cambridge Crystallographic Data Centre comprises H-atom co-ordinates, thermal parameters and remaining bond lengths and angles.

Results and Discussion

Synthesis of Complexes.—The complexes **1**–**4** were synthesised by the reaction of the ligands H$_2$L^1–H$_2$L^4 with cobalt(II) acetate in 1:1 ratio in dimethylformamide in the presence of a 10-fold excess of *N*-methylimidazole (mim). To avoid oxidation to cobalt(III) species all the preparations were carried out under a nitrogen atmosphere. When exposed to air, CHCl$_3$ solutions of **1**–**4** readily take up oxygen and show frozen-glass ESR spectra typical of a Co^{II}–O$_2$ adduct.[14] However, in the solid state, dried samples of **1**–**4** appear to be indefinitely stable to air.

Since the syntheses of **1**–**4** were performed using a large excess of *N*-methylimidazole, the question as to whether five- or six-co-ordinated adducts containing one or two Lewis-base molecules are formed had to be addressed. For the purpose of characterization thermal gravimetric analysis (TGA) was undertaken. The TGA curves revealed a distinct peak corresponding to the loss of *N*-methylimidazole in the temperature range 420–440 K with a weight loss corresponding to only one co-ordinated mim molecule (Table 1). Blank experiments on the four-co-ordinated complexes (*i.e.* containing no axial ligand) showed only the onset of decomposition at 570–620 K.

For Lewis-base adducts of salicylaldiminatocobalt(II) com-

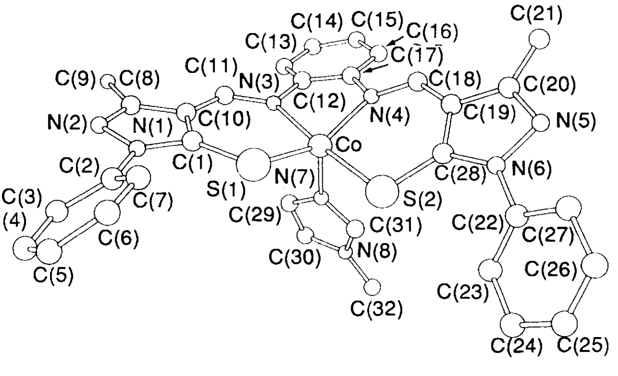

Fig. 1 Molecular structure of compound **4** at 293 K

Table 1 Analytical results for complexes **1**–**4**

		Analysis[a] (%)				
Compound	Colour	C	H	N	S	TGA[a,b] (%)
1	Dark brown	56.0 (56.0)	4.7 (4.7)	18.7 (18.7)	11.6 (10.7)	12.3 (13.7)
2	Light brown	56.4 (56.8)	5.0 (4.9)	18.5 (18.3)	10.7 (10.4)	13.1 (12.8)
3	Light brown	58.45 (58.8)	5.3 (4.9)	16.7 (17.2)	12.6 (12.5)	13.1 (12.5)
4	Brown	58.9 (59.4)	4.6 (4.3)	17.4 (17.3)	9.4 (9.9)	14.7 (13.5)

[a] Calculated values are given in parentheses. [b] Relative mass loss from thermal gravimetry analysis (TGA).

Table 2 Crystal data and details of data collections for complex **4**

	T = 293 K	103 K
a/Å	8.640(2)	8.604(2)
b/Å	9.248(2)	9.124(2)
c/Å	37.228(4)	36.962(4)
β/°	94.66(2)	94.82(2)
U/Å^3	2964.8(9)	2891(1)
D_c/g cm^{-3}	1.45	1.488
μ/cm^{-1}	7.5	7.7
Measured reflections	3061	3218
Observed reflections [$I > 2\sigma(I)$]	1806	2486
θ_{max}/°	25	27
R	0.064	0.049
R' [$w = 1/\sigma^2(F_o)$]	0.052	0.049
S[b]	1.59	1.62

[a] Details in common: formula $C_{32}H_{28}CoN_8S_2$, M = 647.68, crystal size = 0.4 × 0.3 × 0.2 mm, monoclinic, space group $P2_1/c$, Z = 4, $F(000)$ = 1340, λ = 0.7107 Å, ω–2θ scan mode, 228 refined parameters. [b] $S = \Sigma w(|F_o| - |F_c|)^2/(N_o - N_v)$ where N_o is the number of observed reflections and N_p the number of refined parameters.

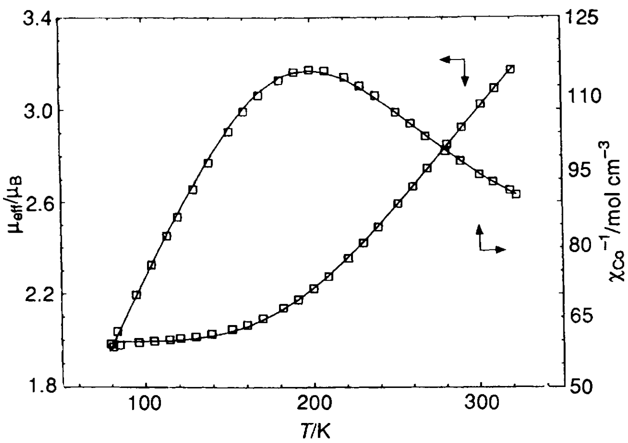

Fig. 2 Magnetic moments and reciprocal susceptibilities *vs.* temperature for compound **1**. Solid lines are calculated with the use of the Martin model (see text)

plexes,[7,15–18] both five- and six-co-ordinated species were isolated in the solid state. The five-co-ordinated complexes appear to be thermodynamically preferred in solution but can also exist in a dynamic equilibrium with six-co-ordinated complexes but only in the presence of a large excess of Lewis base. Predominant formation of the six-co-ordinated species was shown for *N,N'*-bis(3-carboxysalicylidene)ethylenediaminato)cobalt(II) adducts[16] with substituted pyridines. Perhaps this may be interpreted as a result of the electron-withdrawing influence of the carboxylate group, decreasing the electron density on the cobalt atom and facilitating the binding of two donor nitrogen centres.

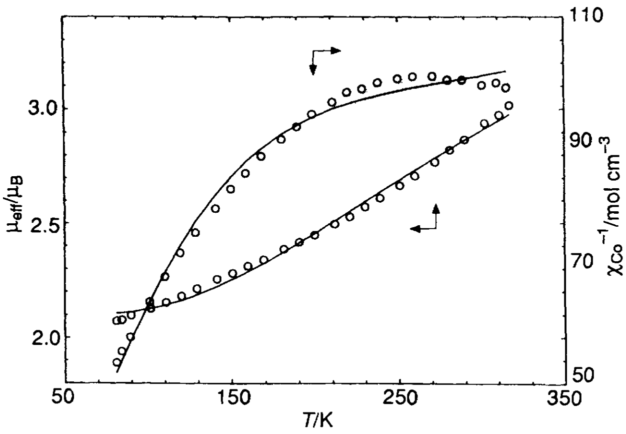

Fig. 3 Magnetic moments and reciprocal susceptibilities *vs.* temperature for compound **2**. Solid lines are calculated with the use of the Martin model (see text)

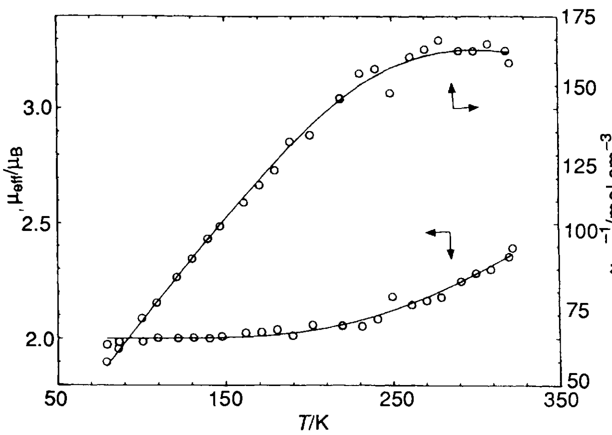

Fig. 4 Magnetic moments and reciprocal susceptibilities *vs.* temperature for compound **3**. Solid lines are calculated with the use of the Martin model (see text)

Magnetic Properties.—The magnetic susceptibility for polycrystalline samples of compounds **1**–**4** was determined in the temperature range 77–320 K. The plots of χ_{Co}^{-1} and μ_{eff} *vs.* T are shown in Figs. 2–5. All of them show a maximum in χ_{Co}^{-1} at the temperature corresponding to the onset of the increase in μ_{eff} from the low-spin state ($S = \frac{1}{2}$) to the high-spin state ($S = \frac{3}{2}$) value. Below this temperature Curie type behaviour is displayed consistent with an occurrence of the low-spin doublet ground state. Spin-crossover proceeds in a gradual manner and is not completed at 320 K.

In order to obtain the enthalpy and entropy of the spin-crossover from the magnetic data we used equation (1) to

Table 3 Fractional atomic coordinates of the non-hydrogen atoms for complex **4** with estimated standard deviations (e.s.d.s) in parentheses

Atom	*x*	*y*	*z*	*x*	*y*	*z*
T = 293 K				103 K		
Co	0.244 0(2)	−0.014 7(2)	0.123 3(4)	0.235 0(2)	−0.010 7(2)	0.125 55(4)
S(1)	0.465 3(3)	0.114 9(3)	0.136 8(1)	0.464 2(3)	0.107 4(4)	0.136 8(1)
S(2)	0.260 5(3)	0.072 5(3)	0.065 2(1)	0.257 8(3)	0.075 9(4)	0.068 5(1)
N(1)	0.661 1(9)	0.137 3(9)	0.198 7(2)	0.662 4(9)	0.131(1)	0.198 8(2)
N(2)	0.680 4(9)	0.096 3(9)	0.234 4(2)	0.682 3(9)	0.088(1)	0.234 9(2)
N(3)	0.215 7(8)	−0.074 3(8)	0.175 5(2)	0.210 8(8)	−0.077(1)	0.175 9(2)
N(4)	0.010 6(8)	−0.018 5(9)	0.121 4(2)	0.006 3(8)	−0.025(1)	0.122 0(2)
N(5)	−0.116(1)	0.235(1)	0.013 3(2)	−0.116(1)	0.237(1)	0.013 5(2)
N(6)	0.041(1)	0.194 2(9)	0.017 9(2)	0.040 2(9)	0.183(1)	0.018 5(2)
N(7)	0.292 0(9)	−0.230 0(9)	0.110 9(2)	0.288 6(9)	−0.228(1)	0.111 2(2)
N(8)	0.311(1)	−0.428(1)	0.079 2(3)	0.310 3(9)	−0.424(1)	0.078 3(3)
C(1)	0.526(1)	0.086(1)	0.181 3(2)	0.526(1)	0.078(1)	0.181 9(3)
C(2)	0.780(1)	0.222(1)	0.184 7(3)	0.783(1)	0.213(1)	0.185 0(3)
C(3)	0.934(1)	0.191(1)	0.197 9(3)	0.938(1)	0.183(1)	0.198 4(3)
C(4)	1.053(1)	0.274(1)	0.184 6(3)	1.059(1)	0.268(1)	0.186 1(3)
C(5)	1.018(1)	0.381(1)	0.160 8(3)	1.024(1)	0.377(1)	0.161 7(3)
C(6)	0.869(1)	0.417(1)	0.149 6(3)	0.875(1)	0.408(1)	0.149 4(3)
C(7)	0.750(1)	0.335(1)	0.161 0(3)	0.753(1)	0.326(1)	0.160 9(3)
C(8)	0.557(1)	0.019(1)	0.239 9(2)	0.555(1)	0.008(2)	0.240 3(3)
C(9)	0.537(1)	−0.047(1)	0.275 4(2)	0.537(1)	−0.056(1)	0.276 5(3)
C(10)	0.455(1)	0.009(1)	0.208 1(2)	0.451(1)	−0.003(1)	0.208 0(2)
C(11)	0.309(1)	−0.060(1)	0.205 3(3)	0.307(1)	−0.069(1)	0.205 5(3)
C(12)	0.065(1)	−0.137(1)	0.178 0(2)	0.063(1)	−0.147(1)	0.178 3(3)
C(13)	0.028(1)	−0.228(1)	0.206 0(3)	0.024(1)	−0.236(1)	0.206 5(3)
C(14)	−0.124(1)	−0.275(1)	0.206 0(3)	−0.127(1)	−0.287(1)	0.207 5(3)
C(15)	−0.234(1)	−0.236(1)	0.179 4(3)	−0.240(1)	−0.251(1)	0.179 9(3)
C(16)	−0.196(1)	−0.152(1)	0.150 7(3)	−0.199(1)	−0.165(1)	0.151 4(3)
C(17)	−0.042(1)	−0.102(1)	0.149 8(2)	−0.048(1)	−0.110(1)	0.150 2(3)
C(18)	−0.089(1)	0.051(1)	0.099 4(3)	−0.095(1)	0.046(1)	0.100 1(3)
C(19)	−0.059(1)	0.121(1)	0.067 4(2)	−0.066(1)	0.123(1)	0.068 5(3)
C(20)	−0.171(1)	0.193(1)	0.043 7(3)	−0.174(1)	0.192(1)	0.043 4(3)
C(21)	−0.338(1)	0.220(1)	0.048 7(3)	−0.346(1)	0.219(1)	0.048 7(3)
C(22)	0.134(1)	0.231(1)	−0.010 8(3)	0.136(1)	0.231(1)	−0.009 8(3)
C(23)	0.259(1)	0.149(1)	−0.017 9(3)	0.267(1)	0.149(1)	−0.016 0(3)
C(24)	0.349(1)	0.196(1)	−0.045 7(3)	0.356(1)	0.195(2)	−0.044 0(4)
C(25)	0.309(1)	0.313(1)	−0.064 3(3)	0.317(1)	0.313(2)	−0.063 7(4)
C(26)	0.186(1)	0.396(1)	−0.057 8(3)	0.190(1)	0.397(2)	−0.057 5(3)
C(27)	0.097(1)	0.354(1)	−0.030 2(3)	0.097(1)	0.353(1)	−0.030 2(3)
C(28)	0.078(1)	0.126(1)	0.049 9(3)	0.074(1)	0.127(1)	0.050 4(3)
C(29)	0.345(1)	−0.339(1)	0.133 0(3)	0.341(1)	−0.344(1)	0.132 9(3)
C(30)	0.355(1)	−0.459(1)	0.113 6(3)	0.359(1)	−0.465(1)	0.112 8(3)
C(31)	0.275(1)	−0.287(1)	0.078 8(3)	0.269(1)	−0.286(1)	0.077 7(3)
C(32)	0.312(1)	−0.520(1)	0.048 1(3)	0.315(1)	−0.519(2)	0.046 5(3)

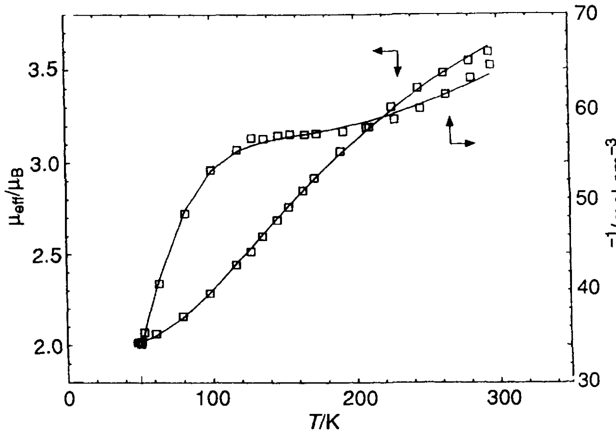

Fig. 5 Magnetic moments and reciprocal susceptibilities *vs.* temperature for compound **4**. Solid lines are calculated with the use of the Martin model (see text)

$$n_{h.s.} = \frac{\mu^2_{expl} - \mu^2_{l.s.}}{\mu^2_{h.s.} - \mu^2_{l.s.}} \qquad (1)$$

estimate the mole fraction of the high-spin form ($n_{h.s.}$), where $\mu_{h.s.}$ and $\mu_{l.s.}$ are the magnetic moments of the high- and low-spin forms ($\mu_{h.s.} = 4.8\ \mu_B$ and $\mu_{l.s.} = 1.9\ \mu_B$)[19] and μ_{expl} is the measured magnetic moment. The equilibrium constant for the low-spin $\rightleftharpoons$ high-spin interconversion was calculated according to equation (2).

$$K = n_{h.s.}/(1 - n_{h.s.}) \qquad (2)$$

From the slope of the linear portion of the ln *K vs.* $1/T$ plots $\Delta H°$ values were estimated and $\Delta S°$ values were determined from the intercept at $1/T = 0$. The thermodynamic parameters obtained are given in Table 6.

The values of $\Delta H°$ listed in Table 6 are close to those reported by Thuery and Zarembovich[18] for six-co-ordinated Lewis-base adducts of Schiff-base complexes with CoO_2N_4 chromophores showing an abrupt transition, $\Delta H° = 1.4–2.3$ kJ mol^{-1}. On the other hand, the $\Delta S°$ values (except that for **1**) are lower and are close to the value implicit due to the spin-multiplicity change alone, $\Delta S°_{spin} = 5.8$ J K^{-1} mol^{-1}. The corresponding five-co-ordinated CoO_2N_3 species[7] display energy separations between low- and high-spin states between 750 and 1300 cm^{-1}, which are higher than those found for **1**–**4** with a CoS_2N_3 chromophore. However, the influence of the replacement of an oxygen by a sulfur in the co-ordination sphere on the energy gap between the high- and low-spin forms can not be deduced

Table 4 Selected bond lengths (Å) and angles (°) for complex **4** with e.s.d.s in parentheses

	T = 293	103 K		T = 293	103 K
Co–S(1)	2.278(3)	2.255(3)	N(6)–C(22)	1.43(1)	1.43(1)
Co–S(2)	2.325(3)	2.277(4)	N(6)–C(28)	1.36(1)	1.33(1)
Co–N(3)	2.055(7)	1.984(8)	N(7)–C(29)	1.36(1)	1.38(1)
Co–N(4)	2.013(7)	1.966(7)	N(7)–C(31)	1.30(1)	1.34(1)
Co–N(7)	2.094(8)	2.117(9)	N(8)–C(30)	1.34(1)	1.36(1)
S(1)–C(1)	1.716(9)	1.73(1)	N(8)–C(31)	1.35(2)	1.31(2)
S(2)–C(28)	1.71(1)	1.73(1)	N(8)–C(32)	1.43(2)	1.46(2)
N(1)–N(2)	1.38(1)	1.38(1)	C(1)–C(10)	1.41(1)	1.41(1)
N(1)–C(1)	1.37(1)	1.37(1)	C(8)–C(9)	1.48(1)	1.48(1)
N(1)–C(2)	1.43(1)	1.41(1)	C(8)–C(10)	1.42(1)	1.43(1)
N(2)–C(8)	1.32(1)	1.35(1)	C(10)–C(11)	1.41(1)	1.38(1)
N(3)–C(11)	1.32(1)		C(12)–C(13)	1.40(1)	1.39(2)
N(3)–C(12)	1.43(1)		C(12)–C(17)	1.38(1)	1.40(1)
N(4)–C(17)	1.41(1)	1. .	C(18)–C(19)	1.40(1)	1.40(2)
N(4)–C(18)	1.31(1)	1.31(1)	C(19)–C(20)	1.42(1)	1.40(2)
N(5)–N(6)	1.41(1)	1.40(1)	C(19)–C(28)	1.40(1)	1.43(1)
N(5)–C(20)	1.32(1)	1.32(1)	C(20)–C(21)	1.50(2)	1.53(2)
S(1)–Co–S(2)	84.8(1)	82.2(1)	S(1)–C(1)–N(1)	125.8(7)	124.7(8)
S(1)–Co–N(3)	95.4(2)	97.5(3)	S(1)–C(1)–C(10)	130.2(7)	128.3(8)
S(1)–Co–N(4)	146.9(2)	154.1(3)	N(1)–C(1)–C(10)	104.0(8)	106.9(9)
S(1)–Co–N(7)	111.8(2)	106.8(3)	N(1)–C(2)–C(3)	116.6(9)	118.0(1)
S(2)–Co–N(3)	174.3(2)	177.2(3)	N(1)–C(2)–C(7)	123.0(9)	122.0(1)
S(2)–Co–N(4)	96.3(2)	97.2(3)	N(2)–C(8)–C(9)	121.1(9)	120.0(9)
S(2)–Co–N(7)	95.5(2)	93.2(3)	N(2)–C(8)–C(10)	111.2(8)	111.6(9)
N(3)–Co–N(4)	80.4(3)	81.9(3)	C(9)–C(8)–C(10)	127.7(9)	128.0(1)
N(3)–Co–N(7)	89.7(3)	89.5(3)	C(1)–C(10)–C(8)	106.4(8)	104.4(9)
N(4)–Co–N(7)	101.0(3)	99.1(3)	C(1)–C(10)–C(11)	128.0(8)	130.0(1)
Co–S(1)–C(1)	108.5(3)	107.3(4)	C(8)–C(10)–C(11)	125.5(8)	125.0(1)
Co–S(2)–C(28)	106.6(4)	107.7(4)	N(3)–C(11)–C(10)	126.0(8)	125.4(9)
N(2)–N(1)–C(1)	113.1(7)	111.9(8)	N(3)–C(12)–C(13)	123.9(8)	125.7(9)
N(2)–N(1)–C(2)	118.0(8)	117.6(8)	N(3)–C(12)–C(17)	114.4(8)	113.9(9)
C(1)–N(1)–C(2)	128.8(8)	130.4(9)	N(4)–C(17)–C(12)	117.4(8)	115.6(9)
N(1)–N(2)–C(8)	105.3(8)	105.1(8)	N(4)–C(17)–C(16)	124.0(8)	126.2(9)
Co–N(3)–C(11)	130.9(6)	130.9(7)	N(4)–C(18)–C(19)	127.0(9)	127.0(1)
Co–N(3)–C(12)	110.3(6)	111.0(6)	C(18)–C(19)–C(20)	125.7(9)	129.0(1)
C(11)–N(3)–C(12)	118.8(8)	118.0(8)	C(18)–C(19)–C(28)	129.6(9)	128.0(1)
Co–N(4)–C(17)	111.4(6)	112.5(6)	C(20)–C(19)–C(28)	104.6(8)	102.5(9)
Co–N(4)–C(10)	128.3(8)	128.2(7)	N(5)–C(20)–C(19)	113.7(9)	115.0(1)
C(17)–N(4)–C(18)	120.2(8)	118.8(9)	N(5)–C(20)–C(21)	118.2(9)	120.0(1)
N(6)–N(5)–C(20)	102.9(8)	103.1(9)	C(19)–C(20)–C(21)	128.0(9)	125.0(1)
N(5)–N(6)–C(22)	116.1(8)	116.2(9)	N(6)–C(22)–C(23)	120.9(9)	121.0(1)
N(5)–N(6)–C(28)	112.8(8)	112.4(9)	N(6)–C(22)–C(27)	118.2(9)	118.0(1)
C(22)–N(6)–C(28)	131.1(8)	131.0(1)	S(2)–C(28)–N(6)	124.9(7)	125.8(8)
Co–N(7)–C(29)	129.6(7)	129.8(7)	S(2)–C(28)–C(19)	129.6(8)	126.5(8)
Co–N(7)–C(31)	125.1(7)	125.7(7)	N(6)–C(28)–C(19)	106.0(8)	107.3(9)
C(29)–N(7)–C(31)	105.3(8)	104.4(9)	N(7)–C(29)–C(30)	109.2(9)	111.0(1)
C(30)–N(8)–C(31)	105.4(9)	110.0(1)	N(8)–C(30)–C(29)	108.2(9)	104.0(1)
C(30)–N(8)–C(32)	128.8(9)	124.0(1)	N(7)–C(31)–N(8)	112.0(9)	110.0(1)
C(31)–N(8)–C(32)	126.0(1)	126.0(1)			

straightforwardly from a comparison of these data since the former values were obtained using a different approach. This approach was based on the crystal-field model of Martin and co-workers[20] developed to interpret the magnetic properties of $[Co(terpy)_2]^{2+}$ complexes. The model assumes an idealized octahedral symmetry and takes into account one ^2E doublet and one $^4T_1$ quartet state separated by energy E. The effects of spin–orbit coupling along with first- and second-order Zeeman interactions removes the degeneracy of the states giving 14 energy levels and the magnetic moment was derived from consideration of the Boltzmann distribution over the 14 levels, equation (3). Here γ is a ligand field parameter for the $^4T_1$ state

$$\mu_{Co}{}^2 = \{150\gamma x C\mu_E{}^2 + 25[\gamma x(5-\gamma)^2 - 20(2-\gamma)^2]\cdot\exp[-(E/\zeta + 5\gamma/6)x] + 2[5\gamma x(11+2\gamma)^2 + 88(2-\gamma)^2]\exp[-(E/\zeta + \gamma/3)x] + 9[35\gamma x(3+\gamma)^2 + 36(2-\gamma)^2]\exp[-(E/\zeta - \gamma/2)x]\}(72\gamma x\{2C + \exp[-(E/\zeta + 5\gamma/6)x] + 2\exp[-(E/\zeta + \gamma/3)x] + 3\exp[-(E/\zeta - \gamma/2)x]\})^{-1} \quad (3)$$

lying between −1.5 for a weak field to −1.0 for strong field; x is ζ/kT where ζ is the one-electron spin–orbit coupling constant: $C \approx Q_E/Q_T$ is the ratio of the vibrational partition functions in the low- and high-spin state and μ_E is the magnetic moment of the low spin state.

In five-co-ordinated Lewis-base adducts of cobalt(II) Schiff-base complexes the ^2E and $^4T_1$ states are split into several doublet and quartet states due to the lower symmetry. It has been suggested[7] that the spin–orbit coupling compensates for the inaccuracy to some extent. A reasonably good fit was obtained.

The best fit least-squares parameters E, μ_E and C for **1**–**4** using

Table 5 Selected angles (°) between the least-squares planes and torsion angles (°) for complex **4**

Plane	Atoms	Angle	T = 293 K	103 K
I	Co, S(1), N(3)			
II	Co, S(2, N(4)	II–I	34.2(8)	26.7(6)
III	S(1), C(1), C(10), C(11), N(3)	III–I	8.7(7)	5.7(6)
IV	S(2), C(28), C(19), C(18), N(4)	IV–II	13.87(66)	14.98(55)
V	Co, N(3), N(4)			
VI	N(3), N(4), C(12), C(17)	VI–V	21.7(7)	19.7(8)
VII	N(1), N(2), C(8), C(10), C(1)	VI–III	1.0(3)	2.5(5)
VIII	C(2), C(3), C(4), C(5), C(6), C(7)	VIII–VII	38.5(4)	37.1(7)
IX	N(5), N(6), C(28), C(19), C(20)	IX–IV	5.3(4)	8.3(4)
X	C(22), C(23), C(24), C(25), C(26), C(27)	X–IX	29.4(5)	29.0(5)
	Torsion angle			
	S(2)–Co–N(7)–C(31)		−21.1(8)	−24.4(8)
	N(3)–Co–N(7)–C(29)		−23.2(9)	−20.6(9)
	N(2)–N(1)–C(2)–C(3)		36(2)	34(2)
	N(5)–N(6)–C(22)–C(27)		31(2)	21(2)
	N(3)–C(12)–C(17)–N(4)		4(2)	7(2)

Table 6 Thermodynamic parameters of the spin equilibria for complexes **1**–**4** and g values for polycrystalline samples at 77 K

Complex	$\Delta H°$/ cm^{-1}	$\Delta S°$/J K^{-1} mol^{-1}	g		
1	757	22.3	2.278	2.059	
2	439	8.6	2.278	2.059	
3	729	8.8	2.253	2.109	
4	273	10.2	2.404	2.183	2.012

Table 7 Best-fit values of E, C and μ_E for the calculated curves in Figs. 2–5 and $T(\chi_{max}^{-1})$

Complex	E/cm^{-1}	C	μ_E/μ_B	$T(\chi_{max}^{-1})$/K
1	1264	0.11	1.95	200
2	921	0.71	2.06	260
3	1428	0.25	1.96	275
4	781	0.46	1.96	125

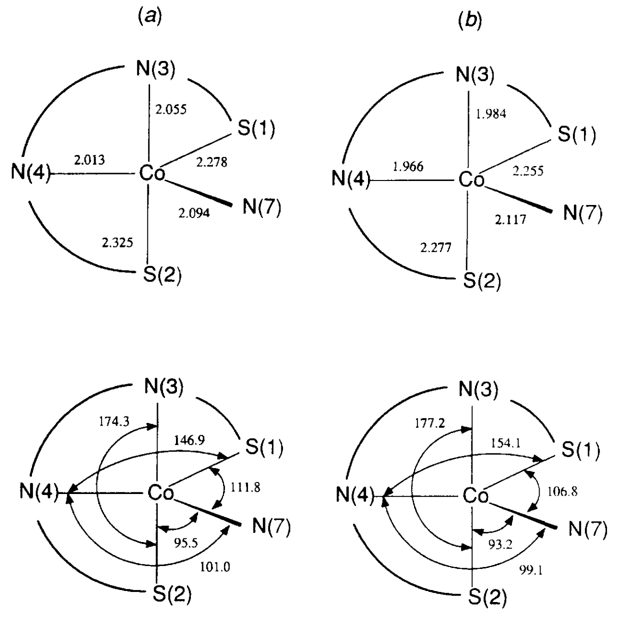

Fig. 6 Schematic representation of the co-ordination polyhedron for compound **4** at (*a*) 293 and (*b*) 103 K with selected bond lengths (Å) and valence angles (°)

the above model (γ was kept constant at -1.5 and ζ held at 475 cm^{-1}) are given in Table 7. The energy separation is obviously overestimated as compared to the data collected in Table 6 which was also shown for the [Co(terpy)$_2$]$^{2+}$ complexes.[21] However, it gives a basis for comparison with the CoO$_2$N$_3$ species.[7] This reveals an increase in the energy gap on going from O to S by 100–200 cm^{-1}. A similar tendency in stabilizing the low-spin state compared to the high-spin ground state of five-co-ordinated cobalt(II) complexes was found by Sacconi[22] in his review of numerous experimental data in which it is shown that lower nucleophilicity of donor atoms favours the formation of high-spin complexes. This is probably the reason why complex **4** derived from the least basic amine precursor reveals the smallest low–high-spin energy separation in the series **1**–**4**. Similar behaviour has been observed[7] for the CoO$_2$N$_3$ complexes.

The powder-EPR spectra of compounds **1**–**4** were recorded at 77 K, no signals being detected at room temperature. The observed g values which span the range 2.012–2.404 are given in Table 6 and may be assigned to the low-spin forms. Complexes **1**–**3** exhibit typical axial spectra[8,16] with $g_{\parallel} < g_{\perp}$ indicating a tetragonal elongation of the co-ordination sphere presumably in a square-pyramidal geometry. The spectrum of **4** shows a distinct rhombic structure with three different g values. The site symmetry of **4** is therefore predicted to be rather low, as confirmed by the X-ray diffraction data (see below).

The Structure of Complex 4.—The X-ray single-crystal molecular structure of **4** was determined at 293 and 103 K. At both temperatures the structure consists of discrete molecules of a five-co-ordinated cobalt(II) centre bound to the two nitrogen and two sulfur atoms of the deprotonated form of the thiopyrazolealdiminato ligand and to the unsubstituted nitrogen atom of the *N*-methylimidazole molecule.

For the sake of clarity and comparison schematic representations of the co-ordination polyhedra at 293 and 103 K with selected bond lengths and angles are shown in Fig. 6. To aid the description of conformational features the selected dihedral and torsion angles are collected in Table 5.

The co-ordination geometry around the cobalt centre is best described as a distorted trigonal bipyramid with the N(3) and S(2) atoms being in axial positions while N(4) and S(1) lie in a basal plane along with the N(7) atom of the *N*-methylimidazole molecule. The cobalt atom is situated almost exactly (within 0.05 Å) in the equatorial plane defined by the S(1), N(4) and N(7) atoms at both temperatures. The N(3), Co and S(2) atoms are close to a collinear alignment with the corresponding valence angle N(3)–Co–S(2) of 174.3(2) (293 K) and 177.2(3)° (103 K). The adoption of a trigonal-bipyramidal structure in the case of **4** is in remarkable contrast to the geometry of [Co(salphen)(2-mim)][H$_2$salphen = *N*,*N*′-bis(salicylidene)-*o*-phenylenediamine, 2-mim = 2-methylimidazole],[7] which displays a square-pyramidal structure. It should be noted that since we are dealing with a chelated tetradentate ligand the formalism developed by Muetterties and Guggenberger[23] for the quantitative discrimination between a trigonal-bipyramidal and alternative square-pyramidal structure in five-co-ordinated complexes of monodentate ligands is not appropriate in this particular case. Thus, to illustrate the difference between the structure of **4** compared to [Co(salphen)(2-mim)], *e.g.* the enlargement of the valence angle N(3)–Co–S(2) compared to the relevant largest N–Co–O angle, 158.8(1)°, by 15.5° (at 293 K) and 18.4° (at 103 K) should be taken into account.

According to the analysis of magnetic behaviour the structure of **4** at 293 K represents an average of approximately 60% of the high-spin form and 40% of the low-spin form. The data do not allow a distinction between a disordered structure and a structure where some sites are in purely low-spin state. In any case the observed changes compared to the low-spin structure represent a lower limit of the actual changes.

The analysis of the structural features of **4** at different temperatures reveals the following essential variations in co-ordination geometry. Compared to the structure at 293 K the valence angle N(3)–Co–S(2) at 103 K increases by 2.9° reflecting a more close approach of the axially ligating atoms to a linear orientation (only 2.8° from the idealized value of 180°). More drastic changes occur in the equatorial plane. The valence angle S(1)–Co–N(4), 146.9(2)°, increases by 7.2° to achieve the value of 154.1° at 103 K. This is accompanied by a decrease of 5.0° in the S(1)–Co–N(7) angle from 111.8(2) to 106.8(3)° and less noticeably a reduction of the N(4)–Co–N(7) angle by 1.9° [101.0(3) and 99.1(3)° at 293 and 103 K], respectively. The changes in the equatorial plane may alternatively be explained in terms of a decrease of the twist angle between the S(1)CoN(3) and S(2)CoN(4) planes [34.2(8)° at 293 K, 26.7(6)° at 103 K], by 7.5°. Similar structural features of the co-ordination polyhedron and their variation with temperature considered as a transformation from distorted square-pyramidal at low-temperature towards a trigonal-bipyramidal arrangement at room temperature were reported for the spin-crossover complex [Co(nnp)(NCS)$_2$].[8]

The Co–N(7) bond in **4** is nearly perpendicular to the N(3) ··· S(2) axis at both temperatures so that the valence angle S(2)–Co–N(7) is 95.5(2) and 93.2(3)°, and N(3)–Co–N(7) is 89.7(3) and 89.5(3)° at 293 and 103 K, respectively. In order to describe the orientation of *N*-methylimidazole group the appropriate torsion angles S(2)–Co–N(3)–C(31) (XI) and N(3)–Co–N(7)–C(29) (XII) may be used. These are deviated by 20–25° from the idealized zero value in the case of parallel alignment of the imidazole ring relative to the S(2)CoN(3) plane, which is higher than the corresponding torsion angles for [Co(salphen)(2-mim)],[7] −6 and −8.9°. The angle XI, −21.1(8) (293 K) and −24.4(8)° (103 K), increases on cooling by 3.3° which is accompanied by a similar decrease of XII, −23.2(9) (293 K) and −20.6(9) (103 K), by 2.6°.

Considering the conformational features of the co-ordinated Schiff-base ligand in **4**, the six-membered chelate ring possess an envelope conformation with a folding along the N(4) ··· S(2), 13.87(66) and 14.98(55)°, and the N(3) ··· S(1) axis, 8.7(7) and 5.7(6)°, at 293 and 103 K, respectively. The envelope conformation is also characteristic of the five-membered chelate ring CoN(3)C(12)C(17)N(4) folded along the N(3) ··· N(4) axis by 21.7(7) (293 K) and 19.7(8)° (103 K). The temperature variation of the above parameters is small and falls in the range of 1–3°. Phenyl groups are twisted by 21–36° relative to the neighbouring pyrazole ring almost independently of the temperature.

The temperature variation is also accompanied by changes in the metal–ligand bond lengths. Those with donor atoms of the Schiff-base ligand increase slightly on heating by 0.02–0.07 Å whereas that with imidazole nitrogen [Co–N(7)] decreases by 0.023 Å. This behaviour may be rationalized as a consequence of the increased population of the in-plane d orbitals in the high-spin form (if a N_2S_2 core of the pyrazole ligand is assumed to be the pseudo-equatorial plane) and strengthening of the ligand field in the axial direction.[6,8] The Co–S bond lengths in **4**, 2.255–2.325 Å, are somewhat larger than those reported for the dimeric [Co(tsalen)] [H$_2$tsalen = *N,N'*-bis(thiosalicylidene)-ethylenediamine][24] 2.20 Å. The Co–N(3) and Co–N(4) bond lengths with nitrogen atoms of the Schiff-base ligand, 1.966–2.055 Å are close to the values revealed[7] for the five-co-ordinated adduct [Co(salphen)(2-mim)], 2.0 and 2.13 Å. The Co–N(7) bond length at the two temperatures lies in the range typical for other Lewis-base adducts of cobalt(II) Schiff-base complexes, 2.07–2.26 Å.[7,25,26]

Acknowledgements

The authors thank F. Jensen for his help with computer software and the Danish Research Council for support.

References

1 P. Gütlich, *Struct. Bonding (Berlin)*, 1981, **44**, 83.
2 E. König, *Prog. Inorg. Chem.*, 1987, **35**, 527.
3 M. Bacci, *Coord. Chem. Rev.*, 1988, **86**, 245.
4 H. Toftlund, *Coord. Chem. Rev.*, 1989, **67**, 108.
5 P. Gütlich and A. Hauser, *Coord. Chem. Rev.*, 1990, **97**, 1.
6 J. Zarembowitch, *New J. Chem.*, 1992, **16**, 255.
7 B. J. Kennedy, G. D. Fallon, B. M. K. C. Gatehouse and K. S. Murray, *Inorg. Chem.*, 1984, **23**, 580.
8 D. Gatteschi, C. A. Ghilardi, A. Orlandini and L. Sacconi, *Inorg. Chem.*, 1978, **17**, 3023.
9 A. B. Orlandini, C. Calabresi, C. A. Ghilardi, P. L. Orioli and L. Sacconi, *J. Chem. Soc., Dalton Trans.*, 1973, 1383.
10 B. N. Figgis, E. S. Kucharski and A. H. White, *Aust. J. Chem.*, 1983, **36**, 1527.
11 J. Josephsen and E. Pedersen, *Inorg. Chem.*, 1977, **16**, 2534; E. Pedersen, *Acta Chem. Scand.*, 1972, **26**, 333.
12 E. A. Boudreaux and L. N. Mulay, in *Theory and Applications of Molecular Paramagnetism*, Wiley, New York, 1976, pp. 491–495.
13 (*a*) G. M. Sheldrick, SHELXS 86, Program for crystal structure determination, University of Göttingen, 1986; (*b*) G. M. Sheldrick, SHELX 76, Program for crystal structure determination, University of Cambridge, 1976.
14 T. D. Smith and J. R. Pilbrow, *Coord. Chem. Rev.*, 1981, **39**, 295.
15 D. Claude, C. W. Schläpfer and A. von Zelewsky, *Struct. Bonding (Berlin)*, 1979, **36**, 129.
16 J. Zarembowitch and O. Kahn, *Inorg. Chem.*, 1984, **23**, 589.
17 R. Morrasi, I. Bertini and L. Sacconi, *Coord. Chem. Rev.*, 1973, **11**, 343.
18 P. Thuery and J. Zarembovich, *Inorg. Chem.*, 1986, **25**, 2001.
19 R. L. Carlin, in *Transition Metal Chemistry*, Marcel Dekker, New York, 1965, vol. 1, p. 1.
20 C. M. Harris, T. N. Lockyer, R. L. Martin, H. R. H. Patil, E. Sinn and I. M. Steward, *Aust. J. Chem.*, 1969, **22**, 2105.
21 S. Kremer, W. Henke and D. Reinen, *Inorg. Chem.*, 1982, **21**, 3013.
22 L. Sacconi, *J. Chem. Soc. A*, 1970, 248.
23 E. L. Muetterties and L. J. Guggenberger, *J. Am. Chem. Soc.*, 1974, **96**, 1748.
24 M. F. Corrigan, K. S. Murray, R. M. Sheahan, B. O. West, G. D. Fallon and B. M. Gatehouse, *Inorg. Nucl. Chem. Lett.*, 1975, **11**, 625.
25 M. Calligaris, D. Minichelli, G. Nardin and L. Randaccio, *J. Chem. Soc. A*, 1970, 2411.
26 P. Charpin, M. Nierlich, D. Vigner, M. Lance, P. Thuery, J. Zarembovich and F. d'Yvoire, *J. Crystallogr. Spectrosc. Res.*, 1988, **18**, 5.

Received 5th July 1993; *Paper* 3/03882C